Quantum Diffusion of H/Ni(111) through a Monte Carlo Wave Function Formalism

S. C. Badescu,[1,2] S. C. Ying,[1] and T. Ala-Nissila[1,2]

[1]Department of Physics, Box 1843, Brown University, Providence, Rhode Island 02912-1843
[2]Helsinki Institute of Physics and Laboratory of Physics, Helsinki University of Technology,
P.O. Box 1100, FIN-02015 HUT Espoo, Finland

We consider a quantum system coupled to a dissipative background with many degrees of freedom using the Monte Carlo wave function method. Instead of dealing with a density matrix which can be very highly dimensional, the method consists of integrating a stochastic Schrödinger equation with a non-Hermitian damping term in the evolution operator, and with random quantum jumps. The method is applied to the diffusion of hydrogen on the Ni(111) surface below 100 K. We show that the recent experimental diffusion data for this system can be understood through an interband activation process, followed by quantum tunneling.

The study of a quantum system coupled to a large background reservoir that leads to thermal fluctuations and dissipation in the dynamical evolution of the system is of central importance in such fields as quantum optics [1], electronic conduction in nanostructures [2], and diffusion of light adatoms on surfaces [3–5]. The standard formalism for this problem is through the master equation for the density matrix $\rho_S(t)$ of the system [3,4]. However, this approach is not practical for condensed matter systems such as a hydrogen adatom moving on a metal surface. In this case, the density matrix would have dimension N^2, where N is the product of the number of sites considered on the surface and the number of vibrational states included at each site. Typically, N would be at least of the order of 10^4, rendering a direct numerical solution of the master equation unfeasible.

Recently, an alternative approach known as the Monte Carlo wave function (MCWF) [1] was developed and applied to solve these types of problems in the field of quantum optics. In the MCWF approach, the evolution of a quantum state $|\Psi(t)\rangle$ is described by a stochastic wave equation, in which the original adiabatic Hamiltonian H_S is only a part of the evolution operator:

$$|\Psi(t + \delta t)\rangle = \frac{f_0}{\sqrt{1 - \delta p}} \exp\left(\frac{-iH\delta t}{\hbar}\right)|\Psi(t)\rangle + \sum_\mu \frac{f_\mu}{\sqrt{\delta p_\mu/\delta t}} C_\mu|\Psi(t)\rangle. \tag{1}$$

Here the effect of each operator C_μ acting on the quantum system represents a collision with the reservoir degrees of freedom that takes the system from one quantum state to another. The new Hamiltonian H is non-Hermitian, built from H_S with an imaginary part added to account for dissipation:

$$H = H_S - \frac{i\hbar}{2}\sum_\mu C_\mu^+ C_\mu. \tag{2}$$

The stochastic nature of quantum evolution is described by the quantities f_0 and f_μ. They are random numbers such that the mean value of f_μ is related to the scattering probabilities

$$\delta p_\mu = \delta t\langle\Psi(t)|C_\mu^+ C_\mu|\Psi(t)\rangle, \tag{3}$$

with $\langle f_\mu\rangle = \delta p_\mu$, and $\langle f_0\rangle = 1 - \delta p$, where $\delta p = \sum p_\mu$ gives the probability for coherent propagation under H. With this choice of dynamics, it can be shown [1] that the quantity $\bar\sigma(t)$, obtained by averaging $\sigma(t) = |\Psi(t)\rangle\langle\Psi(t)|$ over all possible outcomes at time t of the MCWF evolution equation, coincides with the density matrix $\rho_S(t)$ obtained from the solution of the so-called Lindblad form of the master equation [6]:

$$\dot\rho_S = \frac{i}{\hbar}[\rho_S, H_S]$$
$$- \sum_\mu \frac{1}{2}(C_\mu^+ C_\mu\rho_S + \rho_S C_\mu^+ C_\mu - 2C_\mu\rho_S C_\mu^+). \tag{4}$$

The equality between $\bar\sigma$ and ρ_S holds at *all* times t, provided that it holds at $t = 0$. The particular form of the collision operators chosen in Eq. (1) is the most general one that preserves the normalization and positive definiteness of the corresponding $\rho_S(t)$.

It is the purpose of this Letter to demonstrate how the MCWF method can be used to tackle important transport problems in condensed matter physics in cases where the number of degrees of freedom is large enough ($N \gtrsim 10^4$) to make the density matrix approach unfeasible. We consider here the case of a light adatom moving on a metal surface under conditions where the classical activated hopping rate between potential wells is negligible compared with the corresponding tunneling rate. At present, there does not exist a clear consensus on the details of the crossover from the classical activated behavior to the quantum tunneling regime. In the field emission microscopy (FEM) study [7] for Ni and W substrates and in the latest scanning tunneling microscopy study for H/Cu(001) [8], a sharp crossover from classical diffusion to very weak

temperature dependence of diffusion was observed at a temperature in the range of 60–100 K. However, the quasielastic helium atom scattering study for H/Pt(111) [9] yields no crossover down to $T \approx 100$ K. For the H/Ni(111) system, recent optical studies [10] showed a crossover behavior from the classical regime to a *second activated regime* with a lower activation energy below $T \approx 100$ K. This is in contradiction with the FEM data on the same system, which showed a crossover to a temperature independent diffusion at low temperatures [7]. Thus, while there is strong evidence that diffusion proceeds through quantum tunneling at low temperatures, the detailed mechanisms for hydrogen diffusion on different substrates are not yet understood. Previous theoretical works do suggest that the details of the crossover are sensitive to the shape of the adsorption potential and not just determined by the barrier alone [3–5].

We will apply here the MCWF method to study the dynamics of H/Ni(111). The low temperature activated behavior with a barrier of about 90 meV has been attributed to small polaron type activated tunneling [10]. In our view, this is a highly implausible explanation. First, the polaron activation energy for H/Cu(001) [8] was determined to be ~3 meV, then the relaxation energy due to the adatom for H/Ni(001) was calculated to be 2.72 meV [4], and in our recent calculations for H/Pt(111) [11] we also found a relaxation energy of just a few meV; the polaron activation energy is a fraction of the relaxation energy [12]. We will show instead that the data can be explained in terms of tunneling from the first excited vibrational states of the H adatom.

We construct a semi-empirical potential $U(\mathbf{r})$ based on available data as follows. The lowest energy adsorption sites are assumed to be the fcc sites forming a 2D triangular lattice $\{\mathbf{l}\}$ [13] with a lattice constant $a = 2.581$ Å (see Fig. 1). Also, the neighboring hcp sites at a distance of $s = 1.49$ Å [10] are taken to be equal in energy [10] (this is also supported by a recent *ab initio* calculation [14]). Second, we fix the barrier between the fcc and hcp sites close to the value of 196 meV found in experiments [10]. We use the vibrational excitation energy of 94 meV known from [15,16]. $U(\mathbf{r})$ is constructed from localized Gaussians at both the fcc and hcp sites and adjusts the Gaussian parameters, obtaining a fitting with a band gap between the centers of the $A_0 \oplus A_1$ and the $E_0 \oplus E_1$ bands of $\Delta = 96$ meV and a separation between the lowest band and the top of the barrier between fcc and hcp sites of 207 meV.

The adiabatic Hamiltonian H_S for our model is characterized by Bloch states $\{|\mathbf{k}, m\rangle\}$ with corresponding energy $\{\epsilon_{\mathbf{k},m}\}$. Here m is the band index and $\mathbf{k}$ is the 2D wave vector. The center positions and the bandwidths for the first few bands are listed in Table I. The first two branches form 1D representations (A_0 and A_1) of the symmetry group of the 2D triangular lattice, while the next four form 2D representations (E_0 and E_1).

(a)

(b)
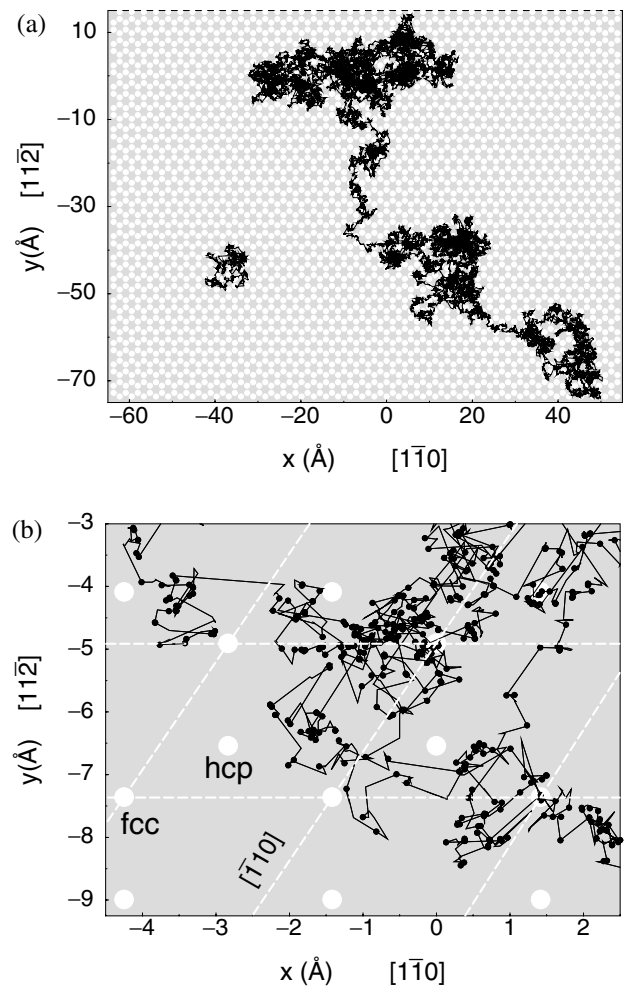
FIG. 1. (a) Trajectories at $T = 70$ K (smaller set) and 110 K (larger set). $\gamma = 1$ and the observation time was 3.1×10^{-2} s. (b) Details of the path at $T = 70$ K. The black circles are excitations or deexcitations. Between two such consecutive points there are usually several random changes of the momentum.

We describe the H adatom as a linear superposition of energy eigenstates:

$$|\Psi(t)\rangle = \sum_{m,\mathbf{k}} b_{\mathbf{k},m}(t) \,|\mathbf{k}, m\rangle, \qquad (5)$$

with $\sum_{m,\mathbf{k}} |b_{\mathbf{k},m}|^2 = 1$. The frictional coupling to the substrate through electronic and phononic excitations is modeled by a general collision operator C_μ (1), through which

TABLE I. Bandwidths $\Delta\epsilon_m$ and band centers ϵ_m for branches 1–6. Groups 1–2 and 3–6 form the composite bands $A_0 \oplus A_1$ and $E_0 \oplus E_1$.

m	$\Delta\epsilon_m$ (meV)	ϵ_m (meV)
1 (A_0)	0.008	104.487
2 (A_1)	0.008	104.497
3 (E_0)	0.017	200.346
6	0.017	200.721
4 (E_1)	0.146	200.446
5	0.146	200.621

we model *both* intraband *and* interband transitions. It is represented as

$$C_{m_1,m_2,\mathbf{q}} = \Gamma_{m_1 m_2,\mathbf{q}}^{1/2} \sum_{\mathbf{k}} |\mathbf{k} + \mathbf{q}, m_1\rangle\langle\mathbf{k}, m_2|, \qquad (6)$$

where Γ is a (yet unspecified) transition rate, and μ in Eq. (1) now becomes a multiple index with two band indices, $\mu = (m_1, m_2, \mathbf{q})$. Thus the probabilities for scattering δp_μ are given by

$$\delta p_\mu = \langle\Psi(t)|C_\mu^+ C_\mu|\Psi(t)\rangle\delta t = \sum_{\mathbf{k}} |b_{\mathbf{k},m_2}|^2 \Gamma_\mu \delta t. \qquad (7)$$

An important feature of the model is that for the low energy bands of interest, $A_0 \oplus A_1$ and $E_0 \oplus E_1$, the composite bandwidths are much smaller than the energy gap Δ separating them (see Table I). This means that we need to consider only two types of transitions: interband transitions between the bands in the two groups and intraband transitions within each group. Since we do not have a microscopic expression for the scattering rates Γ_{intra} and Γ_{inter} we make one further simplification that is $\Gamma_{\text{intra}} = \Gamma_{\text{inter}} = \Gamma$. Below, we will show that the magnitude of D is controlled by the parameter $\gamma = \hbar\Gamma/\Delta_E$, where Δ_E is the width of the upper composite band defined above.

In our numerical calculations, the substrate is represented by a 2D hexagonal box consisting of 180×180 unit cells, with fully periodic boundary conditions. The size of the system is chosen such that the H adatom does not spread outside the boundary during the observation time t. To calculate the spatial $\alpha\beta$ elements of the tracer diffusion coefficient of H, we used the expression

$$D_{\alpha\beta}(t) = \lim_{t\to\infty} \frac{1}{2t}\langle(\hat{x}_\alpha - \langle\hat{x}_\alpha\rangle_0)(\hat{x}_\beta - \langle\hat{x}_\beta\rangle_0)\rangle, \qquad (8)$$

where $\hat{x}$ is the position operator. The average $\langle\cdots\rangle$ in Eq. (8) represents both the quantum mechanical average in a given state as well as the ensemble average over different initial states. Statistical averages to compute D were performed with 1500–6000 initial states, for time intervals containing up to 10^5 collisions. With a code parallelized on four processors, one point on the Arrhenius plot takes 2–4 h, depending on the collision rates.

The symmetry of the lattice implies that the diffusion tensor $D_{\alpha\beta}$ is diagonal. Figure 2 shows the temperature dependence of D for $\gamma = 1, 5$, and 10 on an Arrhenius plot. There is clear activated behavior $D \propto e^{-E_a/k_B T}$, with an activation energy $E_a = 98.1 \pm 0.5$ meV. This is in excellent agreement with the experimental data of Cao *et al.* [10], shown in Fig. 2 as well, in the temperature regime below 100 K, where $E_a \simeq 105$ meV. Obviously, with the inclusion of only the lowest bands in the present calculation, we cannot account for the classical high temperature region above 100 K, where $E_a \simeq 196$ meV [10]. We can give a good qualitative description of the quantum regime, though, where the numerical results above indicate that the observed Arrhenius behavior for D corresponds to *activated quantum tunneling*.
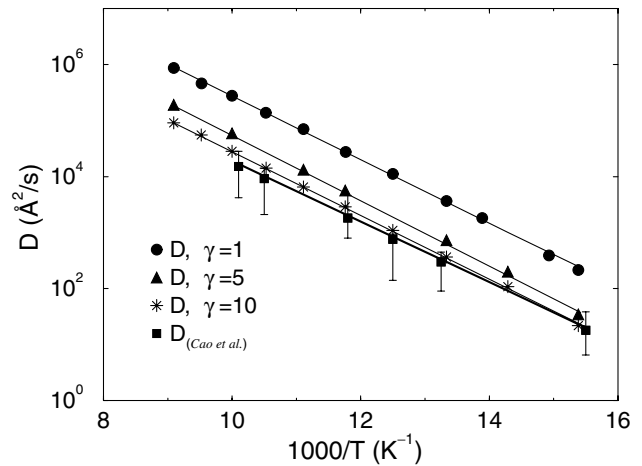
FIG. 2. Temperature dependence of D between 80 and 140 K, for $\gamma = 1, 5, 10$. The Arrhenius behavior is evident. The experimental data of Cao *et al.* [10] are shown for comparison. For $\gamma = 10$, a prefactor D_0 of 2.71×10^9 Å^2/s is obtained. The experimental value of the prefactor D_0 is 2.4×10^9 Å^2/s [10].

The result for the temperature dependence can be understood from the values of the bandwidths listed in Table I. The bandwidths of the $\{E_0, E_1\}$ states are more than 1 order of magnitude larger than for the lower bands (the delocalization was observed also in a recent experiment [15]). Thus, diffusion proceeds mainly via a collision excitation to the upper band, followed by tunneling to neighboring sites and deexcitation to the lower bands again. It is the Bose-Einstein factor $n(\omega)$ ($\hbar\omega = \Delta$), needed to ensure detailed balance in thermal equilibrium [17], that leads naturally to the activated Arrhenius behavior with an activation energy close to the energy gap Δ. Although the Arrhenius behavior of D does not depend on the ratio γ, its absolute magnitude is best fit to the experimental data by choosing $\gamma \approx 10$. This should be taken only as an effective ratio between tunneling and scattering, because, e.g., polaron effects [18,19] which lead to a broadening of the levels and a reduction in the tunneling rate were left out in the present calculation.

The MCWF methods gives insight into the quantum dynamics by allowing one to follow the dynamics of wave packets in real space and time. In Fig. 1 we show two typical trajectories, tracing the evolution of $\langle\hat{\mathbf{r}}\rangle$ for a wave packet. The larger length scale for the trajectory at 110 K reflects the larger value of the diffusion coefficient, which is due to a higher excitation rate into the upper bands. The trajectory at 70 K has points where the particle is in the ground state for a longer time and, by comparison to the trajectory at 110 K, it has less coherent propagation intervals in the upper band. The other point to note is that there are coherent propagation regions with tunneling through several sites before a deexcitation. This can be quantified by studying the tunneling length distribution P_ℓ. We define the tunneling length ℓ as the distance traveled by a wave packet in the upper band before

it suffers a collision. It is found that asymptotically P_ℓ decreases exponentially with ℓ, while it obeys a Poisson-like distribution at small values of ℓ ($\ell \leq s$). This is similar to the jump distribution in the classical regime [20]. Regarding the dependence of D on γ, we have done simulations at $T = 70$ K and $T = 110$ K in the range $0.1 \leq \gamma \leq 10$ and found that $D \propto \gamma^{-1}$ in this range. This inverse power law dependence on γ is similar to the dependence of D on the microscopic friction η in the classical regime [21,22]. However, the influence of the geometrical factor on the dependence of the jump distribution on γ seems rather different from the classical case. The crossover of the dependence on γ or η from quantum to classical behavior is a subject worthy of further investigations.

To summarize, we have demonstrated through a model study of H diffusion on Ni(111) that the MCWF method is a powerful tool in the study of quantum transport problems with many degrees of freedom. In addition, the real space nature of the method allows one to extract interesting information about the dynamics of wave functions, not easily available with other means. As opposed to the small polaron mechanism suggested earlier [10], our results suggest that the low temperature diffusion behavior observed in the work of Cao *et al.* for H/Ni(111) [10] has its origin in the tunneling of the hydrogen adatom from the first vibrational excited state. We plan to apply the same MCWF formalism to investigate other quantum diffusion systems, such as H/Pt(111) [9] and H/Cu(001) [8], which show qualitatively different behaviors from H/Ni(111) [10]. The key is to start with a reliable adsorption potential through a combination of first-principles calculation and empirical inputs.

———————

[1] Y. Castin and K. Mølmer, Phys. Rev. A **54**, 5275 (1996); K. Mølmer, Y. Castin, and J. Dalibard, J. Opt. Soc. Am. B **10**, 524 (1993).

[2] A. Tilke *et al.,* J. Appl. Phys. A **71**, 357 (2000); G. Lang and U. Weiss, Ann. Phys. (Leipzig) **9**, 804 (2000).

[3] H. Metiu and S. Efrima, J. Chem. Phys. **69**, 2286 (1978); D. H. Zhang, J. C. Light, and S. Y. Lee, J. Chem. Phys. **111**, 5741 (1999); V. Pouthier and J. C. Light, J. Chem. Phys. **113**, 1204 (2000).

[4] T. R. Mattsson and G. Wahnström, Phys. Rev. B **56**, 14 944 (1997); T. R. Mattsson, G. Wahnström, L. Bengtsson, and B. Hammer, Phys. Rev. B **56**, 2258 (1997).

[5] L. Y. Chen and S. C. Ying, Phys. Rev. Lett. **73**, 700 (1994).

[6] G. Lindblad, Commun. Math. Phys. **48**, 119 (1976).

[7] T. S. Lin and R. Gomer, Surf. Sci. **225**, 41 (1991).

[8] L. J. Lauhon and W. Ho, Phys. Rev. Lett. **85**, 4566 (2000).

[9] A. P. Graham, A. Menzel, and J. P. Toennies, J. Chem. Phys. **111**, 1676 (1999).

[10] G. X. Cao, E. Nabighian, and X. D. Zhu, Phys. Rev. Lett. **79**, 3696 (1997); A. Wong, A. Lee, and X. D. Zhu, Phys. Rev. B **51**, 4418 (1995).

[11] S. C. Badescu *et al.* (unpublished).

[12] *Hydrogen in Metals III-Properties and Applications,* edited by H. Wipf (Springer-Verlag, Berlin, 1997).

[13] The present assumption of a 2D model should be well justified based on recent evidence that there is no significant mixing between the vertical and horizontal modes, due to the very different characteristic frequencies [15].

[14] G. Kresse and J. Hafner, Surf. Sci. **459**, 287 (2000).

[15] H. Okuyama *et al.,* Phys. Rev. B (to be published).

[16] A. D. Johnson, K. J. Maynard, S. P. Daley, Q. Y. Yang, and S. T. Ceyer, Phys. Rev. Lett. **67**, 927 (1991); H. Yanagita, J. Sakai, T. Aruga, N. Takagi, and M. Nishijima, Phys. Rev. B **56**, 14 952 (1997).

[17] K. Binder, *The Monte Carlo Method in Condensed Matter Physics* (Springer-Verlag, Berlin, 1995).

[18] D. Emin, M. I. Baskes, and W. D. Wilson, Phys. Rev. Lett. **42**, 791 (1979).

[19] C. P. Flynn and A. M. Stoneham, Phys. Rev. B **1**, 3966 (1970).

[20] R. Ferrando, R. Spadacini, and G. E. Tommei, Phys. Rev. E **48**, 2437 (1993); R. Ferrando, F. Montalenti, R. Spadacini, and G. E. Tommei, Phys. Rev. E **61**, 6344 (2000).

[21] H. Risken, *The Hokker-Planck Equation. Methods of Solution and Applications* (Springer-Verlag, Berlin, 1984).

[22] G. Caratti, R. Ferrando, R. Spadacini, and G. E. Tommei, Phys. Rev. E **55**, 4810 (1997); A. Cucchetti and S. C. Ying, Phys. Rev. B **54**, 3300 (1996).